NMR MAGIC ANGLE SAMPLE SPINNING FOR MEASURING WATER AND HEAVY OIL SATURATION AND HIGH RESOLUTION RELAXOMETRY

D. M. Wilson[a] and G. A. LaTorraca[b]

[a]Chevron Research and Technology Company, 100 Chevron Way, Richmond, CA 94802
[b]Chevron Petroleum Technology Company, 1300 South Beach Blvd., La Habra, CA 90631

Abstract

Nuclear magnetic resonance (NMR) relaxometry and/or diffusion measurements can be used to distinguish oil and water fractions in rocks containing low density oils because the relaxation rates and diffusivities of the oil and water are significantly different. However, when core samples contain high density oils, the oil and water relaxation rates are indistinct and diffusion differences too small for straightforward saturation determination. Additionally, high density oils can have complicated T_1 and T_2 distributions as well as a relaxation time constants that are too short to measure with low field relaxometry.

We show the utility of using magic angle spinning (MAS) to remove the susceptibility broadening of the rock matrix, making possible the resolution of the proton chemical shift. We have used MAS measurements to determine water and oil saturations in diatomite samples containing oils with API gravity ranging from ~10 to 27. The MAS measurements yield determinations of the oil and water saturations and estimates of the aromaticity of the oil, and extend relaxometry by obtaining separate T_1's, Carr-Purcell and Hahn-Echo T_2's of oil and water. The relaxation parameters thus obtained are not independent of spinning, and are discussed in the light of the relevant theory regarding MAS and field dependence. The MAS measurements at either 500 or 100 MHz ^{1}H frequencies require only about 150 mg sample with experiment times of a few minutes. Non-MAS spectra of the samples were also acquired at 20 MHz, as were liquid-state spectra of the extracted oils at 500, 100, and 20 MHz.

Introduction

Nuclear magnetic resonance (NMR) is widely used to characterize fluid-saturated oil reservoir cores. One branch of application to petrophysics uses pulsed field gradients to either obtain spatial distribution of fluids (magnetic resonance imaging)[1], or the connectivity and tortuosity of pores (pulse gradient diffusion NMR).[2,3] The older application is the NMR determination of water and oil saturations, free-fluid index, etc., by NMR relaxometry.[4-10] This paper extends the latter application, *via* resolution of the proton chemical shift by magic-angle spinning (MAS). While oil and water fractions in rocks containing low density oils can be separately characterized by traditional low-field (≤ 20 MHz ^{1}H frequency) relaxometry, because the relaxation rates of oil and water are significantly different, the MAS method extends this characterization to core samples containing high density oils which have comparable relaxation rates to water.

NMR relaxometry commonly uses one or more of three diagnostic pulse sequences.[11] An inversion-recovery sequence gives the longitudinal relaxation time T_1, which is dependent upon magnetic fluctuations at approximately the nuclear Larmor frequency, e.g., 20 MHz. A Hahn spin-echo (SE) sequence overcomes microscopic field gradients typical of minerals. SE results are particularly sensitive to lower frequency fluctuations in more viscous samples, as well as molecular diffusion within the microscopic field gradients. Lastly, the Carr-Purcell-Meiboom-Gill (CPMG) sequence takes the SE experiment one step further in eliminating effects of molecular diffusion. The comparison of the two characteristic relaxation times $T_{2,SE}$ and $T_{2,CPMG}$, gives an indication of molecular diffusion.[12]

Conventional high-resolution NMR of mineral samples typically cannot distinguish chemical shift differences of the saturating fluids (e.g., detection of separate oil and water peaks by ^{1}H NMR, <4 ppm of frequency apart), because of the microscopic field gradients. MAS spinning (the "magic angle" is one

inclined arc cos ($3^{-1/2}$) ≈ 54° with respect to the applied external magnetic field, see Figure 1) can reduce or eliminate this interaction. By applying the component pulses of the different diagnostic pulse sequences in synchrony with the MAS spinning frequency, one can extend relaxometry methods to individual components resolved by chemical shift. However, the relaxation parameters thus observed are not necessarily independent of the spinning.[13, 14]

Related papers have appeared using MAS methods on porous minerals: the use of ^{13}C MAS to distinguish macro- and micropores in oil reservoir cores by their relaxation times, which certainly eliminates confusion caused by the presence of water,[15] the demonstration of separate water and oil signals in Berea sandstone saturated with a light crude oil,[16] and ^{1}H relaxation in kaolinite.[13]

Experimental

Materials. Primary samples were from the Lost Hills Diatomite formation, termed Diatomites A (API 19) and B (API 27). Other solid samples used for comparative purposes were Diatomite C and NaY zeolite, which is kept in a controlled humidity environment and is used as a quantitative pore fluid standard. Oil extracts were prepared from the oil cores by Soxhlet extracting approximately 10 g with 250 mL chloroform, followed with Rotovap at 50°C.

Spectroscopy. ^{1}H pulse Fourier transform (FT) spectrometers were used for the measurements, at three different magnetic fields, H_0 = 11.7 T (Bruker MSL), 2.3 T and 0.47 T (Bruker CXP), corresponding to the Larmor frequencies 500, 100, and 20 MHz, respectively. For 500 and 100 MHz NMR measurements of the solids, approximately 120-170 mg of crushed sample was held in a Bruker Instruments 4 mm (O.D.) x 20 mm (length) zirconia rotor. At 20 MHz, approximately the same amount was held in 10 mm Shigemi NMR tubes. The neat (undiluted) oils were held in Wilmad 25 μL spherical microcells, or 5 mm Shigemi NMR tubes. The 20 Mhz spectrometer used a high RF (radiofrequency) homogeneity, low dead time 10 mm probe. π-pulse lengths for all spectrometers were 8 μsec or less. The sample temperature was ambient (21 ± 2°C) in all cases.

Both low- and high-resolution forms of the CPMG sequence were used for the 500 and 100 MHz studies, with π pulses synchronized with MAS spinning (see Figure 2). Only the low resolution method was available at 20 MHz. In high resolution CPMG the number of π pulses is varied, while the recovered signals at the end of the sequences are Fourier transformed to yield high resolution spectra (FT detection). The high resolution spin echo method differs from the CPMG experiment in that a single π pulse is used instead of a train of them. The high resolution T_1 method is the common inversion-recovery sequence, with FT detection. The intensities and shifts of overlapping peaks in the FT spectra were fit using lineshape simulation.[17] All relaxation times were fit with one or more exponentials using PC software.[18]

Results

Figure 3 demonstrates the resolution advantage conferred by MAS, for Diatomite B. Figures 3-6 show some of the high resolution MAS relaxometry data of this sample. Figure 7 is of Diatomite A, showing its higher water content (8.9% vs. 0.8% of whole samples, by weight). Quantitative high resolution CPMG spectroscopy provided oil yields of 8.9% of whole sample, by weight (Diatomite B) and 10.1% (Diatomite A), compared to 8.9 and 8.2%, respectively, by Soxhlet extraction.

Another Lost Hills sample, Diatomite C, had significantly higher magnetic inclusions. Its static spectrum is broader, and the companion 500 MHz ^{1}H, 12 KHz MAS spectrum shows many spinning sidebands at multiples of 12 KHz (Figure 8). Figure 9 shows the 100 MHz ^{1}H, 12 KHz MAS spectrum of the same sample. Because magnetic susceptibility broadening scales with the applied field, the same MAS spinning speed at 1/5 the field barely shows spinning sidebands. However, the resolution of water and oil which is evident in Figure 8 (top spectrum) can only be regained at the lower field by software enhancement (Figure 9, upper spectrum).

Multiexponential fitting[18] yields both amplitudes a^i and relaxation times T^i (where i is the number of components, each with associated relaxation time T^i). A combined relaxation time T^c can be calculated using the equation $1/T^c = \sum_i 1/T^i$. These combined times are given in Tables 1 and 2 for the primary samples.

Of central importance to the study is the effect MAS has on observable relaxometry parameters. Because Diatomite B contains so little water, it is a good sample for comparing oil parameters obtained even at zero spinning speed. Table 3 is a summary of this data, taken at 100 MHz ^{1}H frequency. The high resolution CPMG and spin-echo data were well fit with 2-component decays. Therefore their overall relaxation time, as well as the component set of T^i and a^i are shown.

Discussion

Several issues are relevant to the understanding of this relaxometry data. First, pure liquid ^{1}H relaxation times typically vary with the ^{1}H observation frequency, for viscous liquids. For intramolecular dipolar (^{1}H - ^{1}H, through space) relaxation in an oil molecule undergoing diffusional rotational motion, with characteristic rotational correlation time τ (approximately proportional to the product of macroscopic viscosity and molecular volume at a given temperature[19]) is[20]

$$1/T_1 = C\tau \left[(1 + \omega^2\tau^2)^{-1} + 4 (1 + 4\omega^2\tau^2)^{-1} \right] \quad (1)$$

where C is a constant depending upon the internuclear ^{1}H - ^{1}H distance, and $\omega = 2\pi f$ where f is the ^{1}H Larmor frequency in Hz; and

$$1/T_2 = C\tau/2 \left[3 + 5 (1 + \omega^2\tau^2)^{-1} + 2 (1 + 4\omega^2\tau^2)^{-1} \right] \quad (2)$$

For our purposes we are interested in how relaxation changes with observing ^{1}H frequency. Note that for T_1, if $\omega\tau << 1$, $1/T_1 \approx 5C\tau$; for $\omega\tau >> 1$, $1/T_1 \approx 2C/\omega^2\tau$. Therefore as τ (or viscosity) increases, T_1 first decreases independently of ^{1}H Larmor frequency, but as it goes through a minimum at $\omega\tau \approx 0.6$ and increases, it eventually has a quadratic dependence on ^{1}H frequency, for any given τ.

T_2 changes in a more complicated fashion. It is numerically equal to T_1 for $\omega\tau << 1$; but rather than passing through a minimum with increasing τ, it steadily decreases. In the region $\omega\tau >> 1$ it also increases with ^{1}H frequency, for any given τ.

MAS partially quenches dipolar relaxation and we expect that both T_1 and T_2 could increase with spinning. For T_2 Haeberlen and Waugh have predicted[22], for T_2 in the high viscosity regime $\omega\tau >> 1$

$$1/T_2 = C\tau/2 \left[2 (1 + \omega_r^2\tau^2)^{-1} + (1 + 4\omega_r^2\tau^2)^{-1} \right] \quad (3)$$

where ω_r is the MAS spinning speed. It can be seen that T_2 will have the same limiting value as in (2) for $\omega\tau_r << 1$, but at higher MAS speeds, T_2 will increase and spectral lines of liquids in the high-viscosity regime will narrow.

The foregoing applies to neat liquids. In rocks, new phenomena apply. Surface sites typically contain paramagnetic metal ions, which greatly affect T_1 and T_2, especially of the water component, where for a single pore, the theory of Korringa *et al.*[23], as modified by Kleinberg *et al.*[24,] gives

$$1/T_1 = \rho S/V \quad (4)$$

S and V are the surface area and volume of the pore, and ρ is a relaxivity parameter related to paramagnetic ion site density, fluid-surface distances, etc. However, in the cases of interest here, oil and water are both present in the pores, and water is believed to form a boundary layer between the oil molecules and pore surface, thus mitigating the scalar part of paramagnetic relaxation.[24] Leaving only the dipolar part, T_1 of the oil is more than an order of magnitude larger than that of water,[4] i.e., the surface relaxivity for oil in Equation (4) is much less than for water. However, MAS might still affect T_1 by reducing ^{1}H spin diffusion,[21] causing less efficient relaxation transfer along and between oil molecules, from ^{1}H spins near the paramagnetic sites. Also, the effect of paramagnetic relaxation on T_2 would likely also be different *vis-a-vis* water and oil.

T_2 of fluids in rocks, as measured in CPMG experiments or by MAS, is also affected by microscopic susceptibility differences at the grain-fluid interfaces. These susceptibility differences cause the recovered magnetization in successive CPMG echoes to be reduced, as molecules diffuse from one part of the inhomogeneous magnetic field to another. The addition of this mechanism to that represented by Equations (2) and (4) is

$$1/T_2 = 1/3\ \gamma^2 D G^2 \tau^2 \qquad (5)$$

where 2τ is the spacing between successive π pulses, G the field gradient of the inhomogeneous magnetic field, D the diffusion constant, and γ the nuclear gyromagnetic ratio. It is seen that the extent of this contribution is dependent upon instrumental parameters, as it is more important the higher the field (and thus higher average G), but less if very short pulse spacing can be achieved.

MAS narrows susceptibility-broadened spectral lines, and may also reduce diffusion-broadened ones. Because an induced magnetic field at a paramagnetic site in the rock causes a neighboring dipole field near it with a $3\cos^2\theta - 1$ dependence,[16] all such fields average to zero when θ = arc cos $(3^{-1/2})$. Susceptibility broadening varies linearly with applied field, so to be effective, MAS spinning must be faster than this linewidth.

For SE decay, there is not a simple exponential dependence upon pulse spacing τ, instead the exponent varies[25] as $\gamma^2 D G^2 \tau^3$. The difference between $1/T_{2,\,SE}$ and $1/T_{2,\,CPMG}$, where $1/T_{2,\,se}$ is an overall relaxation rate, may serve to isolate the diffusion/susceptibility mechanism.

Finally, the mechanical effect of MAS should be mentioned. Centrifugal forces may overcome capillary forces and increase diffusion and exchange of molecules between pores.[24]

Applying these principles to the data, first we note the substantial applied field dependence of T_1 of both the oil entrained in the rock and Soxhlet extracted (Tables 1 and 2). This indicates that dipolar relaxation given by Equation (1) dominates T_1 of the oil phase. In Table 3 we find that at a single field strength, MAS lengthens T_1 of the oil, presumably by quenching spin diffusion, but possibly by promoting faster exchange between pores, thus altering S/V in Equation (4). In contrast, T_1 of the water changes little with field, supporting the dominance of surface relaxation, as in Equation (4).

Drawing conclusions from the T_2 data is more difficult. As outlined above, T_2 increases with applied field in the purely dipolar, and dipolar-modified by MAS mechanisms; as well as by MAS overcoming static susceptibility inhomogeneity. On the other hand, T_2 is reduced by increasing applied field, through the diffusion/susceptibility mechanism. The extent of this latter effect on the oil phase may be gauged by comparing the bulk and core sample CPMG and SE data. At 500 and 100 MHz $T_{2,\,CPMG}$ is somewhat greater than $T_{2,\,SE}$, and $T_{2,\,CPMG}$ increases from 20 to 500 MHz ^{1}H frequency for Diatomite B. Table 3 shows that MAS plays very little role when used. But the difference between bulk oil $T_{2,\,CPMG}$ and rock-entrained $T_{2,\,CPMG}$ is approximately an order of magnitude at all fields. This suggests that rather than a predominant diffusion/susceptibility mechanism that would depend quadratically upon the applied field (through G in Equation 5), the dominant T_2 mechanism of oil in pores may be by a surface electron - nuclear relaxation mechanism related to Equation (4). This is certainly true for water. But for the oil phase, the nuclear - nuclear mechanism (Equation 2) may be expressed at higher magnetic fields.

Conclusions

MAS removes the susceptibility broadening of the rock matrix, making possible the resolution of the proton chemical shift. This enables the determination of separate water and oil saturations in diatomite samples, as well as the extension of relaxometry to obtain separate T_1's, Carr-Purcell and Hahn-Echo T_2's of oil and water. The relaxation parameters thus obtained are not independent of spinning, but coupled with variation of applied magnetic field, suggest assignments of the dominant relaxation mechanisms.

References

1. Davies, S., *et al.*, "Quantification of Oil and Water in Preserved Reservoir Rock by NMR Spectroscopy and Imaging," *Magn. Reson. Imaging*, **12**, 349 (1994); Maddinelli, G., and Brancolini, A., "MRI as a Tool for the Study of Water-Flooding Processes in Heterogeneous Cores," *ibid*, **14**, 915 (1996).
2. Hurlimann, M. D., *et al.*, "Restricted Diffusion in Sedimentary Rocks. Determination of Surface-Area-to-Volume Ratio and Surface Relaxivity," *J. Magn. Reson.*, **A111**, 169-178 (1994).
3. "The Influence of Internal Magnetic Field Gradients on NMR Self-Diffusion Measurements of Molecules Adsorbed on Microporous Crstallites," *ibid*, **85**, 381-387 (1989).
4. Latour, L. L., *et al.*, "Nuclear Magnetic Resonance Properties of Rocks at Elevated Temperatures," *J. Colloid Interface Sci.*, **150**, 535-548 (1992).
5. Kleinberg, R. L., *et al.*, "T_1/T_2 Ratio and Frequency Dependence of NMR Relaxation in Porous Sedimentary Rocks," *ibid*, **158**, 195-198 (1993).
6. Kenyon, W. E., "Nuclear Magnetic Resonance as a Petrophysical Measurement," *Nucl. Geophys.* **6**, 153-171 (1992).
7. Peyron, M., *et al.*, "The Modified Stretched-Exponential Model for Characterization of NMR Relaxation in Porous Media," *J. Magn. Reson.* **A118**, 214-220 (1996).
8. Kleinberg, R. L., and Horsfield, M. A., "Transverse Relaxation Processes in Porous Sedimentary Rock," *ibid*, **88**, 9-19 (1990).
9. Lipsicas, M., *et al.*, "Surface Relaxation and Pore Sizes in Rocks - A Nuclear Magnetic Resonance Analysis," *Appl. Phys. Lett.* **48**, 1544-1546 (1986).
10. Morriss, C. E., *et al.*, "Hydrocarbon Saturation and Viscosity Estimation from NMR Logging in the Belridge Diatomite," *SPWLA 35th Symp. 1994;* LaTorraca, G. A., *et al*., "Low Field Determinations of the Properties of Heavy Oils and Water-in-Oil Emulsions," *Magn. Reson. Imaging* **16**, 659 (1998); Brown, R. J. S., "Proton Relaxation in Oils," *Nature* **189**, 387 (1961).
11. Farrar, T. C., and Becker, E. D., "Pulse and Fourier Transform NMR," Academic Press (1971).
12. "^{1}H NMR Study of Water Adsorbed on Carbon Powders," *J. Magn.Reson.* **A109**, 41-45 (1994).
13. Hayashi, S., and Akiba, E., "Nuclear Spin-Lattice Relaxation Mechanisms in Kaolinite Confirmed by Magic-Angle Spinning," *Solid State Nucl. Magn. Reson.*, **4**, 331-340 (1995).
14. Haeberlen, U., and Waugh, J. S., "Spin-Lattice Relaxation in Periodically Perturbed Systems," *Phys. Rev.* **185**, 420-429 (1969).
15. Xiao, L., Du, Y., and Ye, C., "^{13}C Longitudinal Relaxation of Fluids Saturated in Oil Reservoir Cores by MAS NMR," *J. Colloid Interface Sci*. **164**, 495-497 (1994).
16. de Swiet, T. M., Tomaselli, M., Hurlimann, M. D., and Pines, A., "In Situ NMR Analysis of Fluids Contained in Sedimentary Rock," *J. Magn. Reson.* **133**, 385-387 (1998).
17. Bain, A., "Glinfit" (1986).
18. Krider, D., "Superfit" (1988).
19. Bloembergen, N., *et al., Phys. Rev.* **73**, 679-712 (1948).
20. Reference 19, as modified by Kubo, R., and Tomita, K., *J. Phys. Soc. Japan* **9**, 888-919 (1954).
21. Kessmeier, H., and Norberg, R. E., *Phys. Rev.* **155**, 321 (1967).
22. Haeberlen, U., and Waugh, J. S., *Phys. Rev.* **185**, 420-429 (1969).
23. Korringa, J., *et al*., *Phys. Rev.* **127**, 1143 (1962).
24. Kleinberg, R. L., *et al*., *J. Magn.Reson.* **A108**, 206-214 (1994).
25. Carr, H. Y., and Purcell, E. M., *Phys. Rev.* **94**, 630 (1954).

Table 1

Sample & Method All MAS at 12 KHz Spinning		Diatomite B, API 27, 0.8% Water, 8.9% Oil (by Wt) Relaxation Times in Milliseconds		
		500 MHz	100 MHz	20 MHz
T_1 Data	Whole Sample, Water by MAS	5.6	3.0	5.8*
	" " , Oil by MAS	255	46	5.8*
	Extracted Oil	510	85	60
Low-Resolution CPMG Data	Whole Sample, Water and Oil, Non-Spinning	0.59	1.32	0.69*
	Extracted Oil	33	7.0	7.0
High-Resolution CPMG Data	Whole Sample, Water by MAS	0.36	0.84	0.69*
	" " , Oil by MAS	1.40	1.32	0.69*
	Extracted Oil	33	9.1	12.1
Spin-Echo Data	Whole Sample, Water by MAS	0.32	0.92	0.61*
	" " , Oil by MAS	0.91	0.65	0.61*
	Extracted Oil	10.6	10.7	10.4

* Whole sample, combined water and oil, non-spinning.

Table 2

Sample & Method All MAS at 12 KHz Spinning		Diatomite A, API 19, 8.9% Water, 10.1% Oil (by Wt) Relaxation Times in Milliseconds		
		500 MHz	100 MHz	20 MHz
T_1 Data	Whole Sample, Water by MAS	13	10	6.5*
	" " , Oil by MAS	235	85	6.5*
	Extracted Oil	440	110	60
Low-Resolution CPMG Data	Whole Sample, Water and Oil, Non-Spinning	0.38	0.75	1.14*
	Extracted Oil	28	9.8	6.2
High-Resolution CPMG Data	Whole Sample, Water by MAS	1.41	1.16	1.14*
	" " , Oil by MAS	1.10	1.32	1.14*
	Extracted oil	28	8.6	7.0
Spin-Echo Data	Whole Sample, Water by MAS	1.22	0.97	1.03*
	" " , Oil by MAS	0.53	1.02	1.03*
	Extracted Oil	11.5	11.7	6.9

* Whole sample, combined water and oil, non-spinning.

Table 3

	Diatomite B Relaxation Times in Milliseconds Components of 2-Exponential Decays Given as T^i/a^i.		
	12 KHz Spinning	6 KHz Spinning	Stationary
T_1	45.9	43.8	29.6
High-Resolution CPMG	1.32 [0.92/.65, 6.7/.35]	1.26 [0.87/.64, 6.4/.36]	1.28 [0.99/.73, 6.6/.27]
Spin-Echo	0.65 [0.43/.62, 4.3/.38]	0.82 [0.52/.58, 4.3/.42]	0.56 [0.47/.78, 1.6/.22]

Figure 1

Magic Angle Spinning

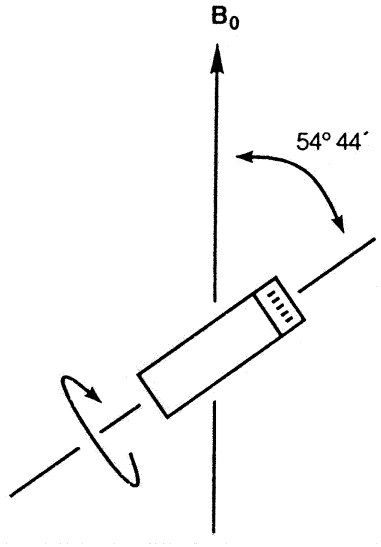

Figure 2

Low-Resolution CPMG

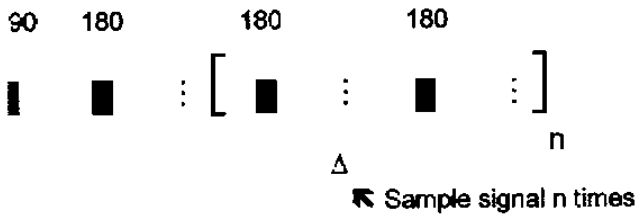

High-Resolution CPMG

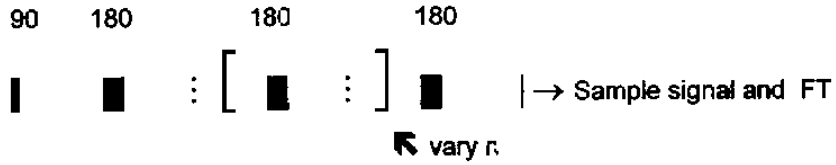

High-Resolution Spin Echo

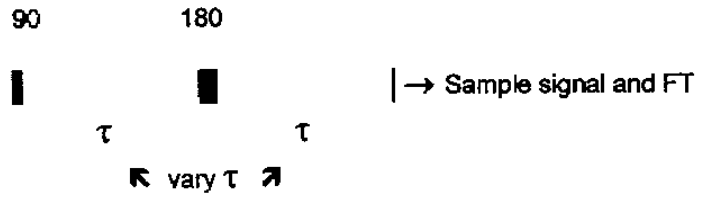

High-Resolution T_1

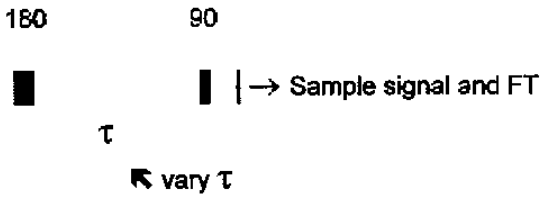

Figure 3

Diatomite B, API 27

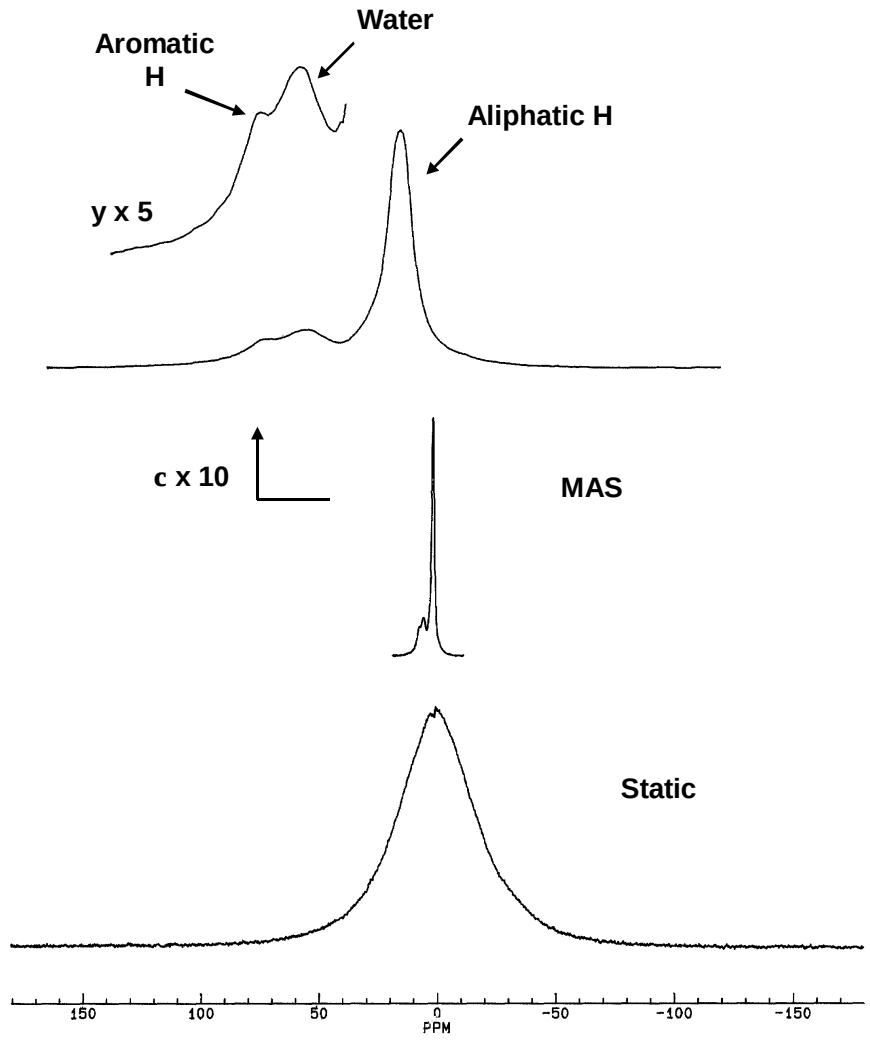

Figure 4

Diatomite B, API 27

T_1 Data

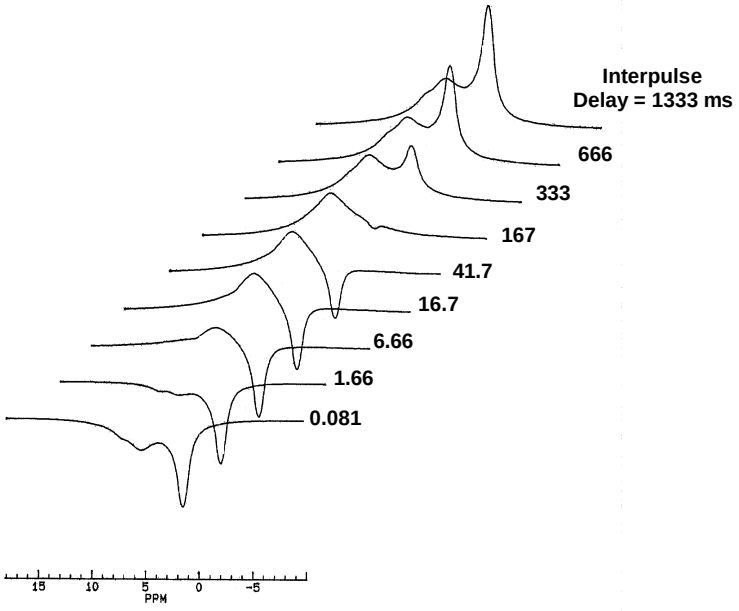

Figure 5

Diatomite B, API 27

Carr-Purcell-Meiboom-Gill High Resolution

1 Cycle = 83.3 m Sec.

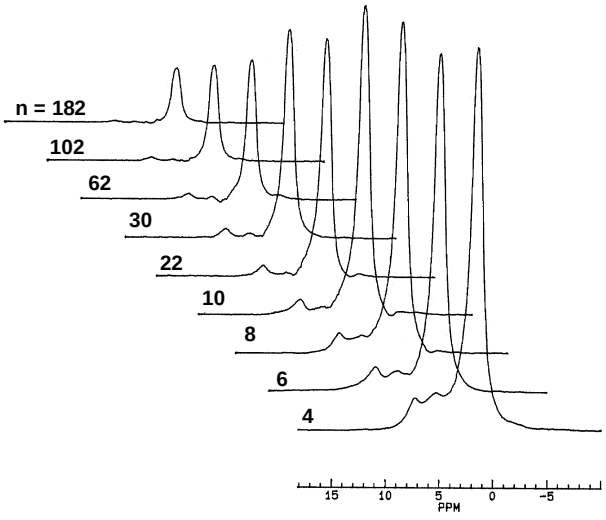

Figure 6

Diatomite B, API 27

Spin Echo Data

1 Cycle = 83.3 m Sec.

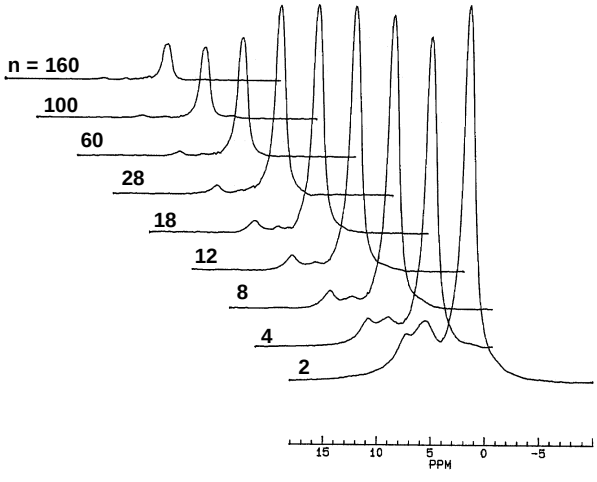

Figure 7

Diatomite A, API 19

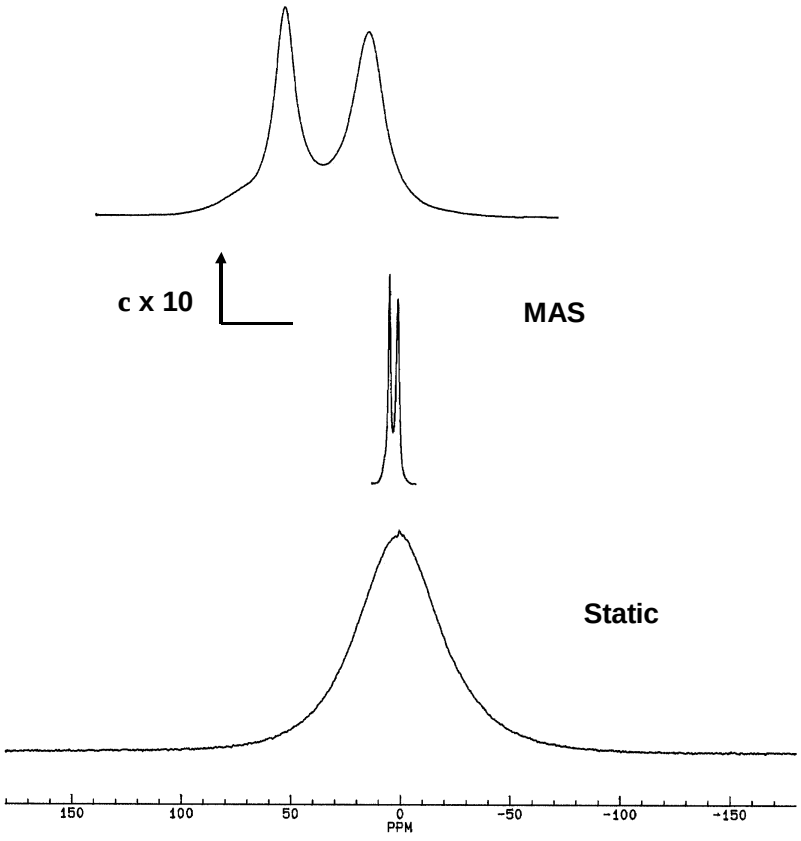

Figure 8

Diatomite C, API 19

500 MHz B_0

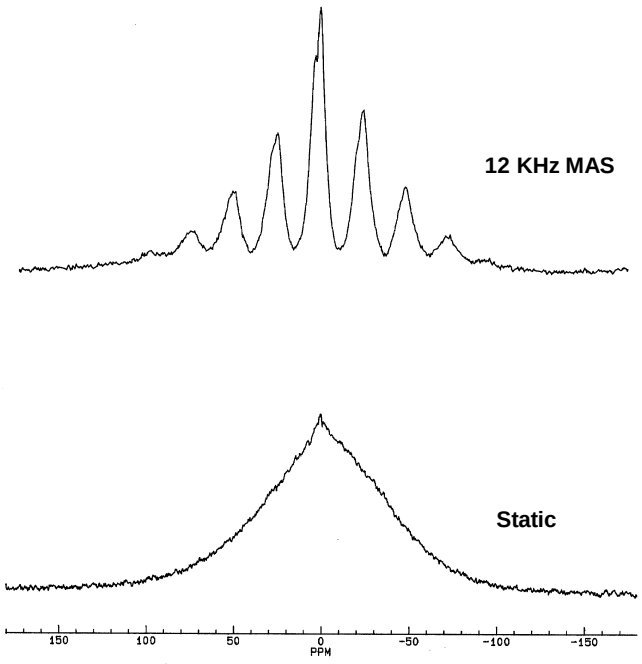

Figure 9

Diatomite C, API 19

100 MHz B_0